Distribution Agreement

In presenting this thesis as a partial fulfillment of the requirements for a degree from Emory University, I hereby grant to Emory University and its agents the non-exclusive license to archive, make accessible, and display my thesis in whole or in part in all forms of media, now or hereafter now, including display on the World Wide Web. I understand that I may select some access restrictions as part of the online submission of this thesis. I retain all ownership rights to the copyright of the thesis. I also retain the right to use in future works (such as articles or books) all or part of this thesis.

Yuming Wen April 8, 2019

Modification of Tetrahydroisoquinoline-and-Mopholine-Containing CXCR4 Antagonists with morpholine analogs

by

Yuming Wen

Dennis C. Liotta, Ph.D.
Adviser

Department of Chemistry

Dennis C. Liotta, Ph.D.

Adviser

Frank E. McDonald, Ph.D.

Committee Member

Gregg M. Orloff, Ph.D.

Committee Member

2019

Modification of Tetrahydroisoquinoline-and-Mopholine-Containing CXCR4 Antagonists with morpholine analogs

By

Yuming Wen

Dennis C. Liotta, Ph.D.

Adviser

An abstract of
a thesis submitted to the Faculty of Emory College of Arts and Sciences
of Emory University in partial fulfillment
of the requirements of the degree of
Bachelor of Sciences with Honors

Department of Chemistry

2019

Abstract

Modification of Tetrahydroisoquinoline-and-Mopholine-Containing CXCR4 Antagonists with morpholine analogs

By Yuming Wen

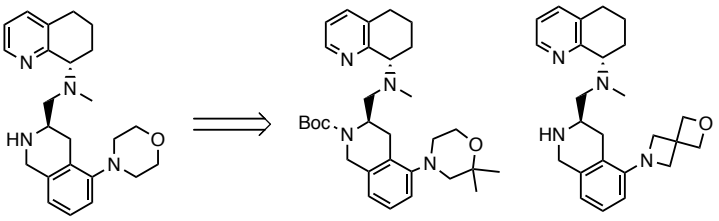

EMU-000172
IC_{50} CXCR4 = 23.8 ± 11.5 nM (Ca^{2+})
= 8.25 ± 4.00 nM (cAMP)
IC_{50} mAChR > 16.7 mM
IC_{50} CYP450 2D6 = 4.28 mM
LM% (H/R/M) = 46/1/1
PAMPA (nm/s) = 438 (pH = 5.5)
= 936 (pH = 7.4)
Caco-2 efflux ratio = 6.11

11b **12**

CXCR4 is a G-protein-coupled receptor that has only one natural ligand, CXCL12. Upon the binding of CXCL12, pathways downstream of CXCR4 such as pro-survival, proliferation, chemotaxis signaling, and transcription of immunosuppressive related genes are triggered. Cancer cells that overexpress CXCR4 can be attracted to CXCL12 rich niches and recruit immunosuppressive leukocytes. Inhibition of CXCR4 with small molecule antagonists can make the cancer cells more susceptible to chemotherapy drugs and the immune system and less likely to metastasize. EMU-000172 is one of a series of tetrahydroisoquinoline-based CXCR4 antagonists developed by Liotta group. It has a good predicted passive diffusion rate but still requires improvement in its off-target effect and metabolic stability. A series of morpholine analogs were chosen to replace the morpholine on EMU-000172. 11b and 12 were the first two to be synthesized. The approaches applied to synthesize 11b suffer from low conversion rates and a large amount of byproducts. However, with a Buchwald-Hartwig amination condition different from those previously used by other group members and a tailored TFA-mediated N-Boc deprotection, the effort to make 12 resulted in a good yield.

Modification of Tetrahydroisoquinoline-and-Mopholine-Containing CXCR4 Antagonists with morpholine analogs

By

Yuming Wen

Dennis C. Liotta, Ph.D.

Adviser

A thesis submitted to the Faculty of Emory College of Arts and Sciences
of Emory University in partial fulfillment
of the requirements of the degree of
Bachelor of Sciences with Honors

Department of Chemistry

2019

Acknowledgements

I would like to foremost thank Dr. Liotta for the opportunity to work in his research laboratory for the past year. I would like to thank Dr. Eric Miller for his mentorship on all aspects of this project. Under his guidance, I acquired not only synthetic organic chemistry skills and medicinal chemistry knowledges but also a true appreciation for the field of medicinal chemistry. I would like to thank Dr. McDonald for the synthetic organic chemistry knowledges and mentorship he granted me both inside and outside of classes. I thank Dr. Orloff for teaching me how fascinating cancer biology is. I would also like to thank all Liotta group members for their time and assistance. Finally, thank you to Dr. Strobel and Dr. Wang for their support in obtaining HRMS and NMR data.

Table of Contents

Introduction

The CXC chemokine receptor type 4 (CXCR4) was discovered to play an important role in T-tropic HIV entry in 1996. The only known ligand of CXCR4 is CXC ligand type 12 (CXCL12, also known as stromal cell-derived factor 1, or SDF-1). Binding of CXCL12 to CXCR4 prevents the virus from binding to the receptor.[1] More recently, scientists discovered that CXCL12/CXCR4 pairing promotes tumor cell proliferation and metastasis. The pro-cancer effects are mediated by interactions with surrounding stromal cells to create a preferable microenvironment. Both the receptor and its ligand are overexpressed by various human cancer types.[2] Methods targeting CXCR4 should be applicable in the treatment of both T-tropic HIV infection and cancer.

CXCR4 is a G-protein-coupled receptor (GPCR), which is widely expressed on the plasma membrane of hematopoietic stem cells, leukocytes, and non-hematopoietic cells including endothelial and epithelial cells.[3] Damaged and hypoxic tissues express CXCR4 as well. When CXCL12 binds to CXCR4, several downstream signaling cascades are triggered to facilitate chemotaxis, cell survival/proliferation, and gene transcription and expression. During the process, Ca^{2+} ions are released and cyclic adenosine monophosphate (cAMP) are generated intracellularly.[4] These two substances may be measured to quantify CXCR4 activity in vitro. CXCL12 is normally secreted by liver, bone marrow, lymph nodes and lungs. Hypoxic and damaged tissue also secrete CXCL12.[5] Tumor cells that overexpress CXCR4 can be attracted to CXCL12 rich sites, where they are surrounded and protected by stromal cells. Tumor cells that metastasize to bone marrow can evade immune recognition and chemotherapy drugs. CXCR4-mediated transcription of angiogenic factors and immunosuppressive cytokines assists tumors in coping with hypoxic environment and cytotoxic agents respectively.[6]

In principle, CXCR4 antagonists can hinder cancer cells' recruitment of

immunosuppressive leukocytes and proangiogenic cells and cancer cells' metastasis to CXCL12 rich regions. Therefore, CXCR4 antagonists can expose cancer cells to patients' immune system and chemotherapy drugs. A variety of CXCR4 antagonists, both small molecules and peptides, has been developed.[7] The bicyclam AMD 3100 represents the first-generation antagonist. It can mobilize hematopoietic stem cells (HSC) from the bone marrow into the circulating blood (Fig. 1).[8] It can also be used in combination therapy to quench the upregulation of CXCR4/CXCL12 caused by the hypoxia, which is induced by cytotoxic agents. However, owing to its cardiotoxicity and poor oral availability,[9] a second generation antagonist (AMD 11070) was created. AMD 11070, though orally available, potently inhibits cytochrome P450 (CYP450) 2D6 and 3A4.[10] Numerous AMD 11070 analogs have since been developed. Some modified the tetrahydroquinoline (THQ) moiety,[11] some altered the butyl amine side chain,[12] and others substituted the benzimidazole moiety.[13] One success among them is GSK812397, which possesses great potency and absorption, distribution, metabolism, and excretion (ADME) profiles (Fig. 1).[14] Other classes of CXCR4 small molecule antagonists such as ITlt contain isothiourea moieties (Fig. 1).[15] Polypeptides like cyclo(-D-Tyr-Arg-Arg-Nal-Ψ-Gly-) may also have a good half maximal inhibitory concentration (IC_{50}) profile (Fig. 1).[16]

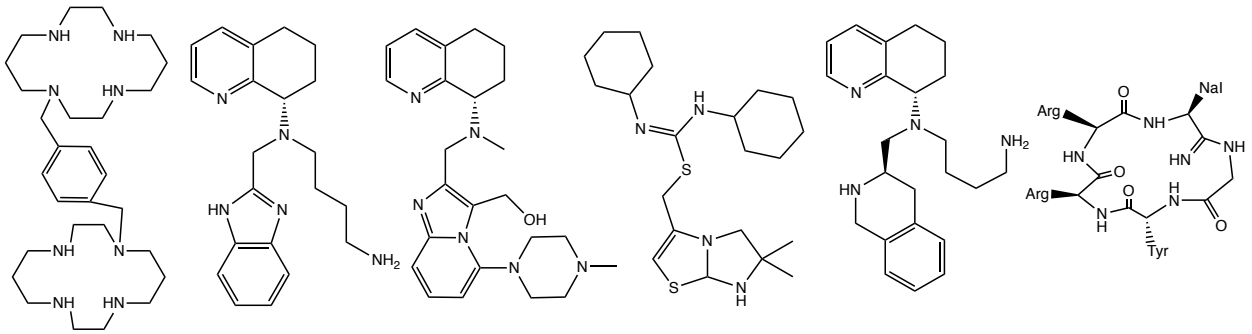

Figure 1. Previously developed small CXCR4 protagonists. Ψ indicates the ψ[-C(=NH)-NH-] substructure. Nal stands for 3-(2-naphthyl)alanine.

The Liotta group designed TIQ-15 based on AMD 11070. The benzimidazole moiety is replaced with a tetraisoquinoline (THIQ) moiety.[17] TIQ-15 is highly potent and selective. However, the Parallel artificial membrane permeability assay (PAMPA) assay predicts that it has poor intestinal permeability (P_c). TIQ-15 also has a very short half-life in mouse liver microsomes. Hence, it is difficult to apply the murine model to study the in vivo efficacy of TIQ-15. Moreover, TIQ-15 inhibits CYP 2D6 at a very low concentration, which restricts its potential usage in combination therapy. Several approaches were taken to improve the ADME property of TIQ-15. The general objectives are reducing the number of rotatable bonds, introducing bulky substituents to hinder CYP binding, increasing lipophilicity, and reducing the number of hydrogen bond donors and the basicity of the amines.[18] Modifications were done to the THQ,[19] the distal amine on the side chain,[20] the side chain,[21,22] and the C-2 position of THIQ.[18] The best of each series is listed in Figure 2.

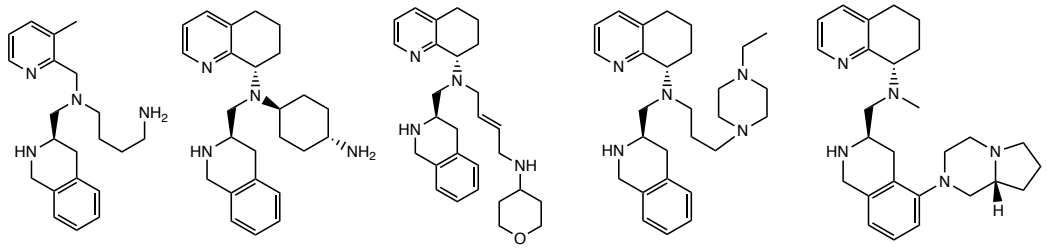

Figure 2. TIQ-15 analogs synthesized previously by the Liotta research group at Emory University.

According to the criteria of target-product profile that were defined: (1) CXCR IC_{50} < 100 nM, (2) muscarinic acetylcholine receptors (mAChR) IC_{50} / CXCR $IC_{50} \geq 1000$, (3) CYP IC_{50} > 20,000 nM, (4) > 50 % in HLM and > 20% in mouse liver microsomes (MLM) remaining, and (5) P_c > 100 nM/s, it was decided that the next step was to change the the substituent on THIQ.

After several heterocycles having been screened, morpholine, instead of the bicyclic

piperazine, was selected to serve as a surrogate for the piperazine on EMU-000034 (Fig. 3) to remove a basic amine, while a hydrogen bond acceptor (HBA) remains. Morphline and its derivatives can be incorporated into the molecule through conventional synthetic pathways.[23] A methyl group was appended to the amine in THIQ of EMU-000172 to increase P_c (Fig. 3). However, the methyl group surprisingly and significantly negatively impacted all ADME results. The dimethyl morpholine in HHN-1-255 completely diminished the CXCR4 binding activity (Fig. 3). Herein, the design and synthesis of EMU-000172 analogs were described.

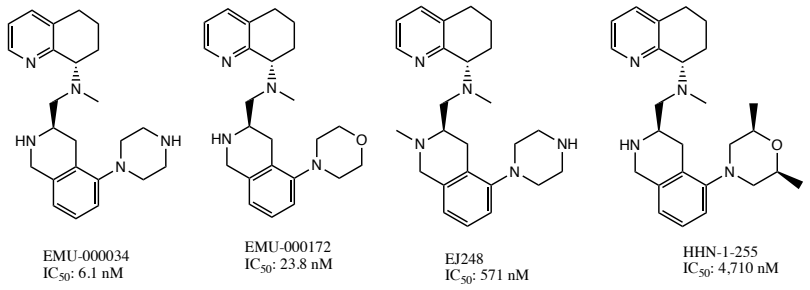

Figure 3. Analogs of EMU-000034 previously synthesized by Liotta group.

Results and discussion

In order to perturb different possible H-bond trajectories, the positions of the oxygen on several morpholine analogs relative to morpholine was analyzed using software by Schrödinger (conducted by Dr. Eric J Miller). The THIQ instead of the whole compound was drawn to reduce variables for the sake of analysis (Fig. 4). In order to increase the stability of EMU-000172 in HLM and reduce its inhibition of CYP450 2D6, the morpholine ring needs to be more rigid. 2-oxa-6-azaspiro[3.3]heptane (1) and 2,2-dimethylmorpholine (2) were chosen as the first to be synthesized. The ring strain of 1 is very high, and it is very rigid. The oxetanyl group of 1 is also known for reducing the rate of metabolic degradation of XXX/by XXX.[24] The two methyl groups on 2 block one of the potentially labile methylene groups and make it difficult for 2 to undergo conformational transitions. Compared with the four methyl groups on the 2,2,6,6-

tetramethylmorpholine, the two methyl groups on 2 would add to 2's lipophilicity but not so much that 2 would become promiscuous and bind to plasma proteins more readily.[25]

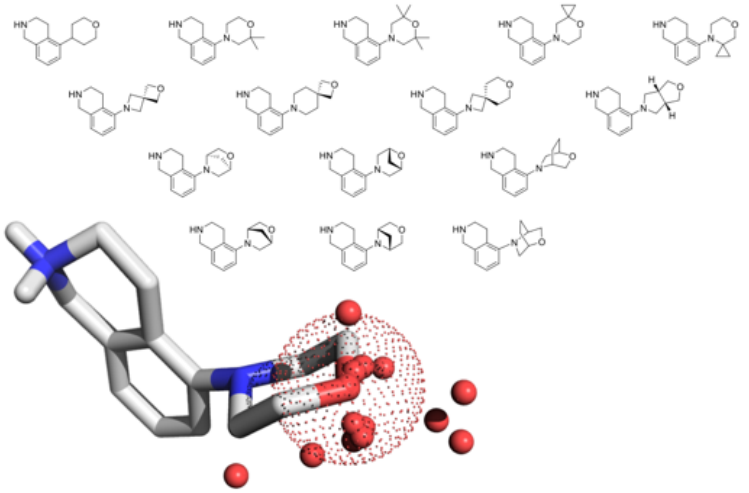

Figure 4. Morpholine analog candidates and the position of their oxygen relative to the original morpholine oxygen. The angle was predicted with SMALL-MOLECULE DRUG DISCOVERY SUITE by Schrödinger. The 3D structure was drawn with PyMOL by Schrödinger.

All synthetic pathways in the Scheme 1 were developed by other members of Liotta group.[18,22] As depicted in scheme 1, the route started with STAB-H-mediated reductive amination of the ketone 3 and the chiral auxiliary amine 4 to provide the amine 5. The directing group on amine 5 was removed with TFA to yield a TFA salt 6. The R-THIQ ester 7, which was previously prepared by other members of the Liotta research group,[18] was reduced with DIBAL-H to furnish the aldehyde 8. The THQ top piece 6 and the THIQ bottom piece 8 was fused via STAB-H-mediated reductive amination to give 9. A methyl group was added onto the none-protected secondary amine of 9 via STAB-H-mediated reductive amination with paraformaldehyde to prepare 10. 10 was utilized as a key intermediate to access a variety of commercially available morpholine analogs through Buchwald–Hartwig amination or Suzuki coupling (Fig. 4).

Scheme 1. Preparation of the key intermediate 10

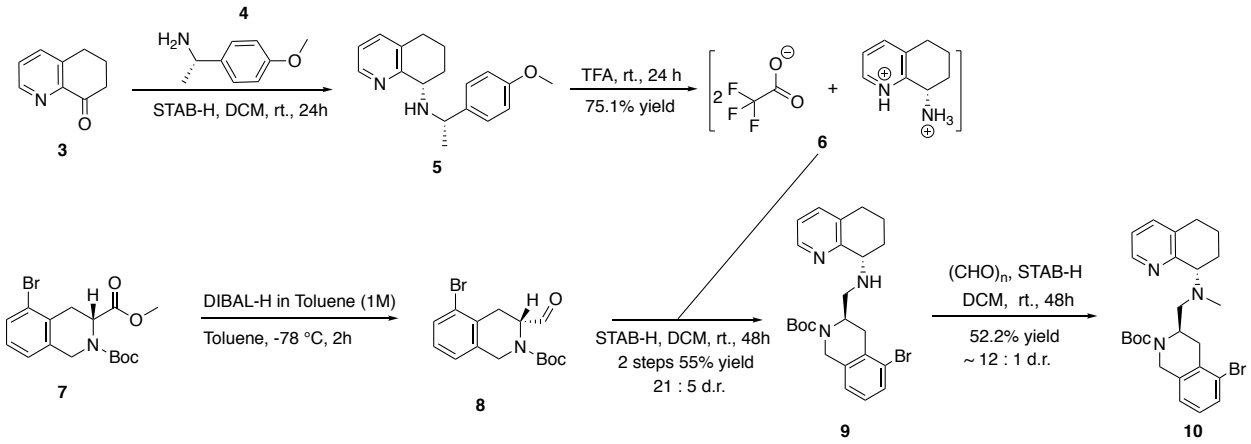

In early efforts to apply Buchwald-Hartwig coupling to append 1 and 2 to 10, poor conversion, a dehalogenated byproduct, and epimerized products were obtained. Several different palladium catalyst systems were tested. Use of Pd $(OAc)_2$, H_2O, XPhos, K_2CO_3, tBuOH at 110 °C [26] and Pd $(dba)_2$, (±)-BINAP, Cs_2CO_3/K_2CO_3, toluene at 120 °C generated poor yields. Strong bases like Na*t*OBu was hypothesized to deprotonate the benzylic hydrogen, which is also alpha to the tertiary amine, on the THQ top piece and gave a large amount of epimerization. For 11a, the G3 Buchwald precatalyst with RuPhos gave perfect conversion and generated very little byproduct and side product. However, for 11b, neither did $Pd_2(dba)_3$ with (±)-BINAP nor did the use of a G3 Buchwald precatalyst with RuPhos result in a good conversion (Scheme 2). The β-hydride elimination of the morpholine analogs was hypothesized to cause the proto-dehalogenation. The ring strain of 1 hampers the lining up of N-C bond with the metal surface, while 2 does not have the ring strain as strong.[28] However, the β-hydride elimination byproducts stemmed from 1 and 2 were not recovered because they are volatile. Meanwhile, the reason why 1 produces so much less epimerization than 2 remains unclear.

Scheme 2. Preparation of 11a and 11b

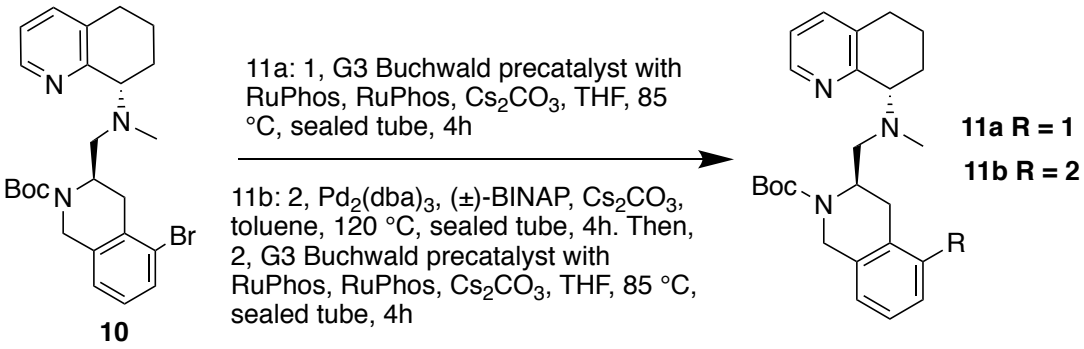

The deprotection of Boc group on 11a with 32 eq. of TFA and a reaction concentration of 0.1M in DCM was first conducted overnight. After workup, the reaction gave an almost 50:50 mixture of product and byproduct. LCMS results show that the byproduct has a mass of (M+18). The byproduct was hypothesized to be the diol 13 derived from ring opening of oxetanyl group.[29] TLC analysis illustrated that not even mobile phase with 5% ammonia hydroxide can stop the product or the byproduct from streaking on the plate. Instead of attempting to isolate the product with reverse phase prep HPLC, the mixture was subjected to a condition of neat TFA at 60 °C under reflux to convert all the product to 13.[29] Unexpectedly, the reaction generated an even mixture of 13 and (M+18) the next day, where M is the mass of 13. The triol 14 derived from azetidine ring opening was hypothesized to be the new byproduct. Meanwhile, the first step of Scheme 3 was conducted again for 5 hours and monitored hourly. The reaction was complete and the percentage of 13 started to accelerate after around two hours. The subsequent Boc deprotection of 11a was run for 1 hour and 15 min because the conversion rate was already at 80% (Scheme 3).

Scheme 3. N-Boc group deprotection of 11a with TFA

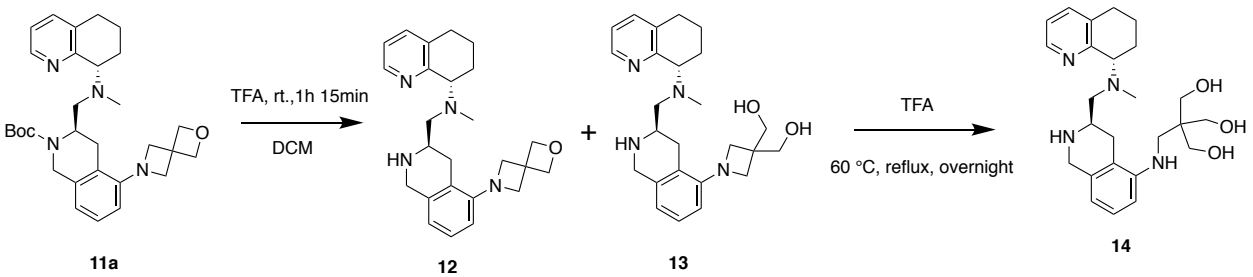

Future work

The in vitro ADME profile of 12 should be established. CXCR4 Ca^{2+} and cAMP flux assays can determine the CXCR4 IC_{50} of 12. The neurotoxicity of 12 can be predicted by mAChR Ca^{2+} assays. CYP Inhibition assays can tell if the rigidity of 1 prevents 12 from binding to CYP. Human and murine liver microsomal stability assays can be used to help people decide if the oxetanyl group improves the metabolic stability of 12 relative to EMU-000172. A PAMPA assay will demonstrate if 12 carries the same good passive diffusion ability of EMU-000172 (Fig. 3). A Caco-2 assay can illustrate if 12 undergoes active efflux by heterogeneous human epithelial colorectal adenocarcinoma cells.

The β-hydride elimination byproducts of 1 and 2 may be recovered in future experiments through distillation. Full characterization of triol 14 and more literature research is required. If the synthesis of 12 is to be scaled up, the amount of the byproduct diol 13 will increase so that 13 may streak and make it harder to isolate the product. In order to limit the amount of oxetanyl ring opening, the molar eq. of TFA used in the N-Boc deprotection may be reduced but to no lower than 5 eq., which is enough to protonate all the basic nitrogens. Experiments can be carried out to determine the relationship between reaction time and eq. of TFA used. With a sensible reaction time in mind, the amount of TFA used can be decided.

The next morpholine analog to be appended on the THIQ should be 7-Oxa-2-Azaspiro[3,5]Nonane (15) (Fig. 4). Under the same condition as 12 was synthesized, 15 should yield a good conversion rate with even less byproduct during the deprotection step because it contains a tetrahydropyran group instead of an oxetanyl group. However, the final product with 15 attached may have a metabolic stability less than that of 12.

Conclusion

Several morpholine analogs were proposed to replace the morhopholine on EMU-000172 to address the CYP 2D6 inhibition and poor murine liver microsomal stability. The addition to the THIQ moiety of two morpholine analogs, 1 and 2 were attempted because both are rigid and 1 contains an oxetanyl group which may improve liver microsomal stability of the compound. However, only the Buchwald-Hartwig amination of 12 gave a good conversion rate and minimal amount of byproducts. For 2, both previously developed Buchwald-Hartwig coupling conditions and newly applied G3 Buchwald precatalyst generate unacceptable amounts of byproducts and have a poor conversion rate. The byproducts were proposed to be due to epimerization of the starting material and product and dehalogenation of the starting material. The dehalogenation was proposed to stem from β-hydride elimination of the morpholine analogs. The TFA-mediated N-Boc deprotection of 12 was run for 1h 15 min instead of overnight to give both as good conversion rate and a minimal amount of byproduct. In vitro and in vivo safety and pharmacokinetics studies of 12 will need to be conducted.

Experimental

General: Automated flash column chromatography was performed using a Teledyne ISCO CombiFlash Companion system with silica gel-packed columns (SiliCycle Inc.). Analytical thin-layer chromatography (TLC, commercially available from Sigma) was carried out on aluminum-supported silica gel plates (thickness: 200 μm) with fluorescent indicator (F-254). Visualization of compounds on TLC plates was accomplished UV light (254 nm) and/or with phosphomolybdic acid, ninhydrin, or ceric ammonium molybdate. NMR spectra (^{1}H, and ^{13}C) were obtained using either a Varian INOVA 600 MHz spectrometer, a Varian INOVA 500 MHz spectrometer, a Varian INOVA 400 MHz spectrometer. NMR samples were prepared and processed in deuterated chloroform ($CDCl_3$) using the residual solvent peak ($CDCl_3$: ^{1}H = 7.26 ppm, ^{13}C = 77.36 ppm) as

an internal reference. NMR data are reported to include chemical shifts (δ) reported in ppm, multiplicities indicated as s (singlet), d (doublet), t (triplet), q (quartet), m (multiplet), coupling constants (J) reported in Hz, and integration normalized to 1 atom (H or C). High resolution mass spectrometry (HRMS) was performed by the Emory University Mass Spectrometry Center, directed by Dr. Fred Strobel. Liquid chromatography-mass spectrometry (LCMS) was performed on an Agilent 1200 HPLC equipped with a 6120 Quadrupole mass spectrometer (ESI-API) eluting at a rate of 1.00 mL/min with mixtures of HPLC grade MeOH and H_2O (all spiked with 0.1% formic acid) through an analytical, reverse-phase, Agilent C18 XDB eclipse column (50 mm x 4.6 mm, 3.5 μM). LCMS samples were prepared in a solution of 50:50 MeOH/H_2O (spiked with 0.1% formic acid), and ultraviolet activity was monitored at 254 nm. Final compound purity was assessed using ^{1}H, ^{13}C NMR, and LCMS.

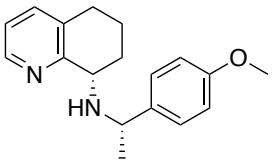

(S)-N-((S)-1-(4-Methoxyphenyl)ethyl)-5,6,7,8-tetrahydroquinolin-8-amine (5):

Sodium triacetoxyborohydride (2.88 g, 13.6 mmol, 2 eq.) was added to a 100 mL flask with a stir bar, diluted with DCM (68 mL), and stirred vigorously at room temperature. 6,7-Dihydroquinolin-8(5H)-one (1 g, 6.8 mmol, 1 eq.) and (S)-1-(4-methoxyphenyl)ethanamine (1.0274 g, 1 mL, 6.8 mmol, 1.00 eq.) were subsequently added, and the resulting brown slurry was allowed to stir vigorously at room temperature overnight. The reaction was quenched with 1 M aqueous sodium hydroxide until pH = 13~14. The aqueous layer was extracted twice with DCM, and the combined organic layers were washed once with brine, dried over anhydrous sodium sulfate, filtered, and evaporated under reduced pressure to yield a mixture of brown solid and yellow crystals.

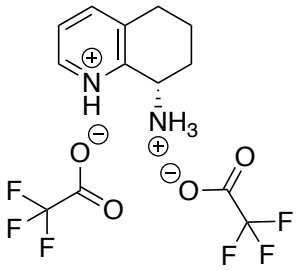

Tert-butyl-(R)-5-bromo-3-formyl-3,4-dihydroisoquinoline-2(1H)-carboxylate (6):

5 (1 g, 3.54 mmol, 1 eq.) was added to a 100 mL flask with a stir bar and diluted with TFA (10.1 mL), which caused the solution to become purple. The resulting reaction mixture was stirred vigorously at room temperature under argon overnight. In the morning, TLC indicated complete conversion of starting material to one major spot. The reaction was quenched with MeOH until the solution become clear yellow. Solvent was evaporated under reduced pressure. The crude material was diluted with 18 mL MeOH, stirred vigorously for 30 min at room temperature, filtered, and the resulting mother liquor was evaporated under reduced pressure. The resulting crude material was diluted with 26 mL hexanes and a small volume of Et_2O. The resulting solution was stirred vigorously at room temperature under Ar for 30 min, decanted, and dried under reduced pressure to yield a fine white powder. The material was dissolved in DCM with a small volume of ether until almost full dissolution was achieved, and left at 0°C for two days. The resulting crystals were filtered, washed with cold hexanes, and dried under vacuum to yield to give clear needles. 1H NMR (500 MHz, $CDCl_3$) δ 8.45 (d, J = 5 Hz, 1H), 7.7 (d, J = 8 Hz, 1H), 7.44 (dd, J = 5 Hz, J = 7.5 Hz, 1H), 7.27 (s, $CDCl_3$), 4.605 (t, J = 6 Hz, 1H), 2.94-2.79 (m, 2H), 3.025 -2.9622 (m, 1H), 2.902-2.845 (m, 1H), 2.387-2.415 (m, 1H), 2.219-2.182 (m, 1H), 2.156-2.128 (m, 1H). LC-MS (ES-API, 10-95 % MeOH in water over 10 min) m/z calculated for $[C9H12N2 + H]^+$ = 149.2, found 149.2.

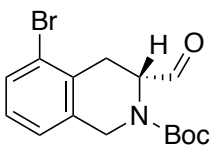

(S)-8-Ammonio-5,6,7,8-tetrahydroquinolin-1-ium-2,2,2-trifluoroacetate (8):

A round bottom flask containing a stir bar was charged with 2-(tert-butyl) 3-

methyl (R)-5-bromo-3,4-dihydroisoquinoline-2,3(1H)-dicarboxylate (0.7 g, 1.89 mmol, 1 eq.) and anhydrous toluene (18.9 mL, 10 eq.). Diisobutylaluminum hydride (1 M solution in toluene, 4.7 mL, 5.6 mmol, 2.96 eq.) was added dropwise at −78 °C. After 2 hours at −78 °C, the reaction was quenched carefully with MeOH (0.23 mL, 5.6 mmol, 2.96 eq.) and then allowed to warm to 0 °C. A saturated solution of Rochelle salt was added, and the mixture was stirred at room temperature for an hour. The biphasic mixture was transferred to a separatory funnel. The aqueous layer was separated and extracted twice with ethyl acetate. The combined organic extract was dried over anhydrous sodium sulfate and concentrated under reduced pressure to afford the title compound (slightly yellow clear oil) as a crude material, which was used for the next step without purification. TLC (1:4, EtOAc:Hex) indicated that no reactant was left. Crude NMR indicated the presence of an aldehyde.

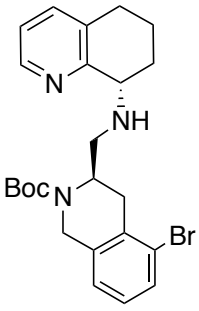

tert-butyl -(R)-5-bromo-3-((((S)-5,6,7,8-tetrahydroquinolin-8-yl)amino)methyl)-3,4-dihydroisoquinoline-2(1H)-carboxylate (9):

A 25 mL round bottom flask equipped with a magnetic stir bar was charged with amine 6 (1 g, 2.66 mmol, 1.41 eq.), STAB-H (0.676 g, 3.19 mmol, 1.69 eq.), and DCM (6.6 mL). After the solution was stirred for 5 min, aldehyde 8 (0.643 g, 1.89 mmol, 1 eq.) dissolved in DCM (2.7 mL) was added in one portion. The resulting mixture was stirred at room temperature for 48h. Upon the completion of the reaction as judged by LC-MS (C18, 25 ~ 95 % MeOH in water over 6 min). The mixture was quenched with 1 M NaOH. The TLC (1:20, MeOH:DCM) indicated that there was no reactant left. The biphasic mixture (pinkish color) was transferred to a separatory funnel. The aqueous layer was separated and extracted with DCM two times. The combined organic extract was dried over anhydrous sodium sulfate and

concentrated under reduced pressure to a crude material (clear reddish pink, 0.9 g), which was purified by a CombiFlash system (25 g RediSep Rf GOLD silica column, eluent A: DCM and eluent B: MEOH; 0~2 min 0% B; 2~15 min, 0~5% B; 15~20 min, 5% B, 20~30 min, 5~20% B) to afford the Boc-protected product. 1H NMR (500 MHz, CDCl3): δ 8.37 (d, J = 35 Hz, 1H), 7.460 -7.358 (m, 2H), 7.06 (d, J = 6 Hz, 3H), 4.893-4.56 (m, 2H), 4.242 (d, J = 16 Hz, 1H), 3.775-3.696 (m, 1H), 3.178-3.145 (d, J = 19 Hz, 1H), 2.957-2.592 (m, 7H). LC-MS, (m/z): calculated for $[C_{24}H_{30}BrN_3O_2 + H]^+$ = 472.16, 473.15, 474.15, 475.16, found: 472.2, 473.2, 474.0, 475.2.

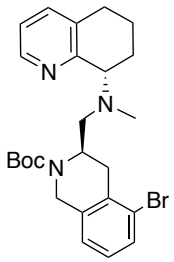

tert-butyl (R)-5-bromo-3-((methyl((S)-5,6,7,8-tetrahydroquinolin-8-yl)amino)methyl)-3,4-dihydroisoquinoline-2(1H)-carboxylate (10):

A round bottom flask equipped with a magnetic stir bar was charged with amine 9 (1 eq.) in DCM (0.1 M), and dropwise STAB-H (1.8 eq.). After the solution was stirred for 5 min, paraformaldehyde (3 eq.) was added in one portion. The resulting mixture was stirred at room temperature for 48h. The reaction was quenched with 1M NaOH. The aqueous layer was extracted twice with DCM. Combine organic layers were washed once with brine and dried over anhydrous sodium sulfate, filtered, and evaporated under reduced pressure. However, the reaction did not go to completion after 48h according to TLC and LC-MS after workup. A MS peak of 473.2 ($[9 + H]^+$) suggested the presence of starting material. Hence, the material was resubjected to reaction condition amount of paraformaldehyde, DCM and STAB-H. After another 48h, the reaction went to completion. Both TLC and LC-MS (25 ~ 95 % MeOH in water over 8 min) results suggested the presence of diastereomers (d.r. ≈ 1:1). The diastereomers have a R_f of around 0.4 in a TLC system of 1:15 (MeOH:DCM). LC-MS (m/z): calculated for $[C_{25}H_{32}BrN_3O_2 + H]^+$ = 486.17, 487.17, 488.17, 489. 17, found: 488.2, 489.2. The second

workup gave a mixture of 427 mg of diastereomers. The mixture was purified by a CombiFlash system (30 g RediSep Rf GOLD silica column, eluent A: DCM and eluent B: MEOH; 0~3 min, 0% B; 2~15 min, 0~5% B; 15~20 min, 5% B; 20~30 min, 5~25 %B) three times to yield 265 mg of the target diastereomer. ^{1}H NMR (500 MHz, $CDCl_3$): δ 8.416 (d, J = 4 Hz, 1H), 8.271 (s, 1H), 7.35 (d, J = 4.5 Hz, 1H), 7.31 (s, 1H), 7.138 (q, J = 5 Hz, J = 8 Hz, 1H), 6.991-6.967 (m, 3H), 4.913-4.518 (m, 2H), 4.192-4.157 (m, 1H), 3.71 (s, 1H), 2.989 (m, 1H), 2.765 (m, 2H), 2.639-2.18 (m, 7H), 1.985-1.81 (m, 5H), 1.643-1.568 (m, 1H), 1.528-1.407 (m, 10H), 1.359-1.202 (m, 1H).

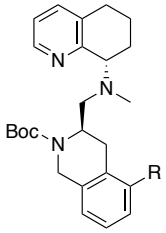

11a R = 1
11b R = 2

tert-butyl (*R*)-3-((methyl((*S*)-5,6,7,8-tetrahydroquinolin-8-yl)amino)methyl)-5-(2-oxa-6-azaspiro[3.3]heptan-6-yl)-3,4-dihydroisoquinoline-2(1*H*)-carboxylate (11a): 500 mg of 10 (1 eq.) was added to an oven-dried microwave vial with a stir bar. Added [2-(2-aminophenyl)phenyl]-methylsulfonyloxy-palladium; dicyclohexyl-[2-(2,6- diisopropoxyphenyl)phenyl]phosphane (0.01 eq.), 2-Dicyclohexylphosphino-2',6'-di-i-propoxy-1,1'-biphenyl (0.01 eq.), and cesium carbonate (1.2 eq.) in succession. The tube was then sealed with a microwave vial cap. The resulting mixture was evacuated under reduced pressure and subsequently flushed with Ar. This two step procedure was repeated twice more. 1 (1.2 eq.) was weighed out in an oven-dried and degassed LCMS vial. Degassed THF was added to the LCMS vial. The 1 in THF was transferred to the microwave vial and the resulting mixture was sonicated and then stirred vigorously under Ar for 5 min to mix well the solid with the solution. The resulting reaction mixture (1 M) was stirred vigorously at 85 °C for 4 hrs. The reaction mixture was then cooled to room temperature and filtered over a plug of celite, which was subsequently washed with EtOAc. The resulting mother liquor was evaporated under reduced pressure to yield a yellow oil of 619 mg. LCMS shows a crude relative area

percentages of 11a : 10 : protodehalogenation byproduct (BP) = 69.2% : 29.4% : 1.5%. 1.04% of 11a epimerized. The reaction mixture after workup was resubjected to reaction condition with 0.05 equivalence of precatalyst and the ligand. The workup with same method conferred a yellow foam of 641 mg. The crude material was purified with column chromatography (CombiFlash, 40 g column, 30 min): solvent A = DCM; solvent B = MeOH; 0~3 min, 0% B; 3~20 min, 0~7% B; 20~25 min, 7~9% B; 25~30 min, 9~25% B) to yield a white foam of 370 mg (73.4% yield). 1H NMR for 12 (600 MHz, $CDCl_3$) δ 8.244 (d, J = 17.8, 1H), 7.23 (d, J = 5.76, 1H), 6.96 (t, J = 7.74, 1H), 6.9 (d, J = 2.4, 1H), 6.38-6.5 (m, 1H), 6.27 (d, J = 7.92, 1H), 4.8-4.89 (m, 7H), 4.4-4.7 (m, 3H), 4.16 (d, J = 7.5, 3H), 3.87 (d, J = 7.5, 4H), 3.7-3.93 (m, 2H), 2.55-2.85 (m, 6H), 2.2-2.45 (m, 6H), 1.87-1.98 (m, 3H), 1.72-1.84 (m, 2H), 1.55-1.64 (m, 2H), 1.49 (s, 1H). LCMS (ESI-API) 50-95% MeOH in H_2O, 6 min, m/z = 505.3 (M + H), t = 2.75 min. . LCMS also shows a crude relative area percentages of 11a : 10 : BP = 98.6% : ND : 1.7% with 1.3% of the product epimerized.

tert-butyl (*R*)-5-(2,2-dimethylmorpholino)-3-((methyl((*S*)-5,6,7,8-tetrahydroquinolin-8-yl)amino)methyl)-3,4-dihydroisoquinoline-2(1*H*)-carboxylate (11b): 400 mg of 10 (1 eq.) was added to an oven-dried microwave vial with a stir bar. Added [2-(2-aminophenyl)phenyl]-methylsulfonyloxy-palladium; dicyclohexyl-[2-(2,6- diisopropoxyphenyl)phenyl]phosphane (0.05 eq.), 2-Dicyclohexylphosphino-2',6'-di-i-propoxy-1,1'-biphenyl (0.05 eq.), and cesium carbonate in succession. The tube was then sealed with a microwave vial cap. The resulting mixture was evacuated under reduced pressure and subsequently flushed with Ar. This two step procedure was repeated twice more. 2 (1.2 eq.) was weighed out in an oven-dried and degassed LCMS vial. Degassed THF was added to the LCMS vial. The 2 in THF was transferred to the microwave vial and the resulting mixture was sonicated and then stirred vigorously under Ar for 5min to mix well the solids with the solution. The resulting reaction mixture was stirred vigorously

at 85 °C for 4 hrs. The reaction mixture was then cooled to room temperature and filtered over a plug of celite, which was subsequently washed with EtOAc. The resulting mother liquor was evaporated under reduced pressure to yield a yellow oil. The reaction mixture after workup was subjected to another catalyst system that consists of $Pd_2(dba)_3$ (0.05 eq.), (RS)-2,2'-bis(diphenylphosphino)-1,1'-binaphthyl (0.05 eq.), and cesium carbonate (1.2 eq.). The same procedure was repeated except that the solvent was toluene (0.8 M) and the reaction temperature was 120 °C. LCMS shows a crude relative area percentages of 11b : 10 : PB = 7% : 46.4% : 20.5% with 18.5% of the product epimerized. LCMS (ESI-API) 50-95% MeOH in H_2O, 6 min, m/z = 521.3 (M + H), t = 3.8 min. LCMS also shows a crude relative area percentages of 11b : 10 : PB = 4% : 71.2% :23.2% with 3.9% of the product epimerized.

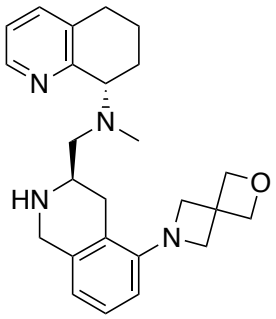

(*S*)-*N*-(((*R*)-5-(2-oxa-6-azaspiro[3.3]heptan-6-yl)-1,2,3,4-tetrahydroisoquinolin-3-yl)methyl)-*N*-methyl-5,6,7,8-tetrahydroquinolin-8-amine (12): A solution of spiral morpholine product 11a (360 mg, 1 eq.) in DCM (0.1 M) was added to a 250 mL round bottom flask with a stir bar. Added 2,2,2-trifluoroacetic acid (32 eq.), and the resulting reaction mixture was stirred vigorously at room temperature under Ar for an hour and 15 min. The reaction mixture was quenched with 1M aqueous sodium hydroxide until the pH reached 13-14. The resulting aqueous layer was extracted 3 times with DCM, and combined organic layers were dried over Na2SO4, filtered, and evaporated under reduced pressure to yield 293 mg of yellow oil. The crude material was purified via combiflash (0 ~ 100% DCM/(90:10:5, DCM:MeOH:NH4OH)). The fractions were concentrated to afford the title compound (219 mg, 75 % yield) as a white foam and 13 (20 mg) as a white foam as well. ^{1}H NMR for 12 (600 MHz, $CDCl_3$) δ 8.46 (dd, J = 1.56,

9.36 Hz, 1H), 7.33 (dt, J = 0.72, 5.64 Hz, 1H), 7.05 (dd, J = 4.68, 7.68 Hz, 1H), 6.99 (t, J = 7.8 Hz, 1H), 6.54 (d, J = 7.56 Hz, 1H), 6.29 (d, J = 7.86 Hz, 1H), 4.796 (q, J = 6.36 Hz, 6H), 4.08 (d, J = 7.44, 3H), 3.83-4.02 (m, 7H), 2.64-2.82 (m, 6H), 2.5 (s, 5H), 2.4-2.49 (m, 2H), 2.13 (d, J = 10.56, 1H), 2.1 (d, J = 10.44, 1H), 1.65-1.75 (m, 1). ^{13}C NMR for 12 (600 MHz, $CDCl_3$) δ 172.59, 158.1, 149.42, 146.92, 136.79, 136.65, 133.87, 125.78, 123.22, 121.59, 118.49, 110.51, 81.24, 64.41, 62.79, 59.93, 59.9, 51.64, 48.98, 41.66, 38.78, 31.45, 29.3, 26.18, 21.38. HRMS (NSI) m/z: $[M+H]^+$ calcd for $C_{25}H_{32}N_4OH$ 405.26; found 405.26510.

^{1}H NMR for 13 (600 MHz, $CDCl_3$) δ 8.445 (d, J = 4.08 Hz, 1H), 7.35 (d, J = 7.56, 1H), 7.06 (dd, J = 4.74, 9 Hz, 1H), 6.99 (t, J = 7.8 Hz, 1H), 6.525 (d, J = 7.56, 1H), 6.17 (d, J = 7.92, 1H), 3.79-4.02 (m, 7H), 3.67 (d, J = 12, 3H), 3.555 (d, J = 6, 3H), 3.355 (d, J = 6.96, 3H), 2.84 (m, 6H), 2.40-2.51 (m, 7H), 2.148 (dd, J = 10.74, 15.54 Hz), 1.96-2.09 (m, 3H), 1.87-1.96 (m, 1H) 1.65-1.75 (m, 1H). ^{13}C NMR for 13 (500 MHz, $CDCl_3$) δ 157.9, 150.2, 147.2, 137.29, 134.44, 126.28, 122.63, 122.07, 118.09, 110.9, 67.77, 64.8, 59.93, 58.53, 51.85, 48.99, 40.79, 39.81, 31.35, 29.65, 25.01, 21.7 (NMR sample was very dilute because only 20 mg of 12 was made). HRMS (NSI) m/z: $[M+H]^+$ calcd for $C_{25}H_{34}N_4O_2H$ 423.27; found 423.27561.

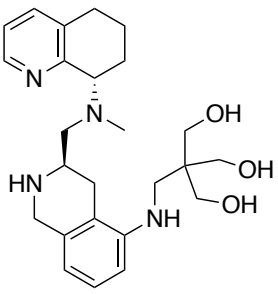

2-(hydroxymethyl)-2-((((*R*)-3-((methyl((*S*)-5,6,7,8-tetrahydroquinolin-8-yl)amino)methyl)-1,2,3,4-tetrahydroisoquinolin-5-yl)amino)methyl)propane-1,3-diol (14) (hypothesized structure): A solution of spiral morpholine product 11a (46 mg, 1 eq.) in DCM was added to a 5 mL round bottom flask with a stir bar. Added 2,2,2-trifluoroacetic acid (37 eq.) and water (2 eq.), and the resulting reaction mixture was stirred vigorously at 60 °C under Ar overnight under reflux. The reaction mixture was quenched with 1M aqueous sodium hydroxide until the pH

reached 13-14. The resulting aqueous layer was extracted 3 times with DCM, and combined organic layers were dried over Na_2SO_4, filtered, and evaporated under reduced pressure. LCMS (ESI-API) 50-95% MeOH in H2O, 6 min, m/z = 221.2 (M/2 + H), 441.3 (M + H), t = 2.29 min. LCMS shows a crude relative area percentages of 13 : 14 = 56.4% : 43.6%.

References

(1) Oberlin, E.; Amara, A.; Bachelerie, F.; Bessia, C.; Virelizier, J.-L.; Arenzana-Seisdedos, F.; Schwartz, O.; Heard, J.-M.; Clark-Lewis, I.; Legler, D. F.; Loetscher, M.; Baggiolini, M.; Moser, B. Erratum: The CXC Chemokine SDF-1 Is the Ligand for LESTR/Fusin and Prevents Infection by T-Cell-Line-Adapted HIV-1. *Nature* **1996**, *384*(6606), 288–288.

(2) Guo, F.; Wang, Y.; Liu, J.; Mok, S. C.; Xue, F.; Zhang, W. CXCL12/CXCR4: a Symbiotic Bridge Linking Cancer Cells and Their Stromal Neighbors in Oncogenic Communication Networks. *Oncogene* **2016**, *35*, 816−826.

(3) Murdoch, C. CXCR4: chemokine receptor extraordinaire. *Immunological Reviews* **2000** *177*, 175-184.

(4) Teicher, B. A.; Fricker, S. P. CXCL12 (SDF-1)/CXCR4 Pathway in Cancer. *Clin. Cancer Res.* **2010**, *16* (11), 2927−2931

(5) Kucia, M.; Jankowski, K.; Reca, R.; Wysoczynski, M.; Bandura, L.; Allendorf, D. J.; Zhang, J.; Ratajczak, J.; Ratajczak, M. Z. CXCR4-SDF- 1 Signalling, Locomotion, Chemotaxis and Adhesion. *J. Mol. Histol.* **2003**, *35*, 233−245.

(6) Righi, E.; Kashiwagi, S.; Yuan, J.; Santosuosso, M.; Leblanc, P.; Ingraham, R.; Forbes, B.; Edelblute, B.; Collette, B.; Xing, D.; Kowalski, M.; Mingari, M. C.; Vianello, F.; Birrer, M.; Orsulic, S.; Dranoff, G.; Poznansky, M. C. CXCL12/CXCR4 Blockade Induces Multimodal Antitumor Effects That Prolong Survival in an Immunocompetent Mouse Model of Ovarian Cancer. *Cancer Research* **2011**, *71*(16), 5522–5534.

(7) Debnath, B.; Xu, S.; Grande, F.; Garofalo, A.; Neamati, N. Small Molecule Inhibitors of CXCR4. *Theranostics* **2013**, *3*, 47−75.

(8) De Clercq, E. The AMD3100 Story: The Path to the Discovery of a Stem Cell Mobilizer (Mozobil). *Biochem. Pharmacol.* **2009**, *77*, 1655−1664.

(9) Chen, Y.; Ramjiawan, R. R.; Reiberger, T.; Ng, M. R.; Hato, T.; Huang, Y.; Ochiai, H.; Kitahara, S.; Unan, E. C.; Reddy, T. P.; Fan, C.; Huang, P.; Bardeesy, N.; Zhu, A. X.; Jain, R. K.; Duda, D. G. CXCR4 Inhibition in Tumor Microenvironment Facilitates Anti-Programmed Death Receptor-1 Immunotherapy in Sorafenib-Treated Hepatocel- lular Carcinoma in Mice. *Hepatology* **2015**, *61*, 1591−1602.

(10) Nyunt, M. M.; Becker, S.; Macfarland, R. T.; Chee, P.; Scarborough, R.; Everts, S.; Calandra, G. B.; Hendrix, C. W. Pharmacokinetic Effect of AMD070, an Oral CXCR4 Antagonist, on CYP3A4 and CYP2D6 Substrates Midazolam and Dextromethorphan in Healthy Volunteers. *JAIDS, J. Acquired Immune Defic. Syndr.* **2008**, *47* (5), 559−565.

(11) Skerlj, R.; Bridger, G.; McEachern, E.; Harwig, C.; Smith, C.; Wilson, T.; Veale, D.; Yee, H.; Crawford, J.; Skupinska, K.; Wauthy, R.; Yang, W.; Zhu, Y.; Bogucki, D.; Di Fluri, M.; Langille, J.; Huskens, D.; De Clercq, E.; Schols, D. Synthesis and SAR of Novel CXCR4 Antagonists That Are Potent Inhibitors of T-Tropic (X4) HIV-1 Replication. *Bioorg. Med. Chem. Lett.* **2011**, *21*, 262−266.

(12) Skerlj, R. T.; Bridger, G. J.; Kaller, A.; McEachern, E. J.; Crawford, J. B.; Zhou, Y.; Atsma, B.; Langille, J.; Nan, S.; Veale, D.; Wilson, T.; Harwig, C.; Hatse, S.; Princen, K.; De Clercq, E.; Schols, D. Discovery of Novel Small Molecule Orally Bioavailable C-X-C Chemokine Receptor 4 Antagonists That Are Potent Inhibitors of T- Tropic (X4) HIV-1 Replication. *J. Med. Chem.* **2010**, *53* (8), 3376− 3388.

(13) Miller, J. F.; Gudmundsson, K. S.; D'Aurora Richardson, L.; Jenkinson, S.; Spaltenstein, A.; Thomson, M.; Wheelan, P. Synthesis and SAR of Novel Isoquinoline CXCR4 Antagonists with Potent Anti- HIV Activity. *Bioorg. Med. Chem. Lett.* **2010**, *20*, 3026−3030.

(14) Jenkinson, S.; Thomson, M.; McCoy, D.; Edelstein, M.; Danehower, S.; Lawrence, W.; Wheelan, P.; Spaltenstein, A.; Gudmundsson, K. Blockade of X4-Tropic HIV-1 Cellular Entry by GSK812397, a Potent Noncompetitive CXCR4 Receptor Antagonist. *Antimicrob. Agents Chemother.* **2010**, *54* (2), 817−824.

(15) Thoma, G.; Streiff, M. B.; Kovarik, J.; Glickman, F.; Wagner, T.; Beerli, C.; Zerwes, H. G. Orally Bioavailable Isothioureas Block Function of the Chemokine Receptor CXCR4 in Vitro and in Vivo. *J. Med. Chem.* **2008**, *51*, 7915−7920.

(16) Inokuchi, E.; Oishi, S.; Kubo, T.; Ohno, H.; Shimura, K.; Matsuoka, M.; Fujii, N. Potent CXCR4 Antagonists Containing Amidine Type Peptide Bond Isosteres. *ACS Medicinal Chemistry Letters* **2011**, *2*(6), 477–480.

(17) Truax, V. M.; Zhao, H.; Katzman, B. M.; Prosser, A. R.; Alcaraz, A. A.; Saindane, M. T.; Howard, R. B.; Culver, D.; Arrendale, R. F.; Gruddanti, P. R.; Evers, T. J.; Natchus, M. G.; Snyder, J. P.; Liotta, D. C.; Wilson, L. J. Discovery of Tetrahydroisoquinoline-Based CXCR4 Antagonists. *ACS Medicinal Chemistry Letters* **2013**, *4*(11), 1025–1030.

(18) Nguyen, H. H.; Kim, M. B.; Wilson, R. J.; Butch, C. J.; Kuo, K. M.; Miller, E. J.; Tahirovic, Y. A.; Jecs, E.; Truax, V. M.; Wang, T.; Sum, C. S.; Cvijic, M. E.; Schroeder, G. M.; Wilson, L. J.; Liotta, D. C. Design, Synthesis, and Pharmacological Evaluation of Second-Generation Tetrahydroisoquinoline-Based CXCR4 Antagonists with Favorable ADME Properties. *Journal of Medicinal Chemistry* **2018**, *61*(16), 7168–7188.

(19) Wilson, R. J.; Jecs, E.; Miller, E. J.; Nguyen, H. H.; Tahirovic, Y. A.; Truax, V. M.; Kim, M. B.; Kuo, K. M.; Wang, T.; Sum, C. S.; Cvijic, M. E.; Paiva, A. A.; Schroeder, G. M.; Wilson, L. J.; Liotta, D. C. Synthesis and SAR of 1,2,3,4-Tetrahydroisoquinoline-Based CXCR4 Antagonists. *ACS Medicinal Chemistry Letters* **2017**, *9*(1), 17–22.

(20) Tahirovic, Y. A.; Truax, V. M.; Wilson, R. J.; Jecs, E.; Nguyen, H. H.; Miller, E. J.; Kim, M. B.; Kuo, K. M.; Wang, T.; Sum, C. S.; Cvijic, M. E.; Schroeder, G. M.; Wilson, L. J.; Liotta, D. C. Discovery of N-Alkyl Piperazine Side Chain Based CXCR4 Antagonists with Improved Drug-like Properties. *ACS Medicinal Chemistry Letters* **2018**, *9*(5), 446–451.

(21) Jecs, E.; Miller, E. J.; Wilson, R. J.; Nguyen, H. H.; Tahirovic, Y. A.; Katzman, B. M.; Truax, V. M.; Kim, M. B.; Kuo, K. M.; Wang, T.; Sum, C. S.; Cvijic, M. E.; Schroeder, G. M.; Wilson, L. J.; Liotta, D. C. Synthesis of Novel Tetrahydroisoquinoline CXCR4 Antagonists with Rigidified Side-Chains. *ACS Medicinal Chemistry Letters* **2018**, *9*(2), 89–93.

(22) Miller, E. J.; Jecs, E.; Truax, V. M.; Katzman, B. M.; Tahirovic, Y. A.; Wilson, R. J.; Kuo, K. M.; Kim, M. B.; Nguyen, H. H.; Saindane, M. T.; Zhao, H.; Wang, T.; Sum, C. S.; Cvijic, M. E.; Schroeder, G. M.; Wilson, L. J.; Liotta, D. C. Discovery of Tetrahydroisoquinoline-Containing CXCR4 Antagonists with Improved in Vitro ADMET Properties. *Journal of Medicinal Chemistry* **2018**, *61*(3), 946–979.

(23) Rupak, K.; Vulichi, S. R.; Suman, K. Emphasizing morpholine and its derivatives (MAID): A typical candidates of pharmaceutical importance. *Int. J. Chem. Sci.* **2016**, *14*(3), 1777-88.

(24) Wuitschik, G.; Carreira, E. M.; Wagner Björn; Fischer, H.; Parrilla, I.; Schuler, F.; Rogers-Evans, M.; Müller Klaus. Oxetanes in Drug Discovery: Structural and Synthetic Insights. *Journal of Medicinal Chemistry* **2010**, *53*(8), 3227–3246.

(25) Leeson, P. D.; Springthorpe, B. The Influence of Drug-like Concepts on Decision-Making in Medicinal Chemistry. *Nature Reviews Drug Discovery* **2007**, *6*(11), 881–890.

(26) Fors, B. P.; Krattiger, P.; Strieter, E.; Buchwald, S. L. ChemInform Abstract: Water-Mediated Catalyst Preactivation: An Efficient Protocol for C-N Cross-Coupling Reactions. *ChemInform* **2008**, *39*(51).

(27) Bruno, N. C.; Tudge, M. T.; Buchwald, S. L. Design and Preparation of New Palladium Precatalysts for C–C and C–N Cross-Coupling Reactions. *Chem. Sci.* **2013**, *4* (3), 916–920.

(28) Teplyakov, A. V.; Bent, B. E. ChemInform Abstract: β-Hydride Elimination from Alkyl and Cycloalkyl Groups on a Cu(100) Surface: Ring Strain and Planarity of the Transition State. *ChemInform* **2010**, *27* (7).

(29) Camerino, M. A.; Zhong, N.; Dong, A.; Dickson, B. M.; James, L. I.; Baughman, B. M.; Norris, J. L.; Kireev, D. B.; Janzen, W. P.; Arrowsmith, C. H.; Frye, S. V. The Structure–Activity Relationships of L3MBTL3 Inhibitors: Flexibility of the Dimer Interface. *MedChemComm* **2013**, *4* (11), 1501.